

Mössbauer-effect study of Fe_2TiO_5 , an anisotropic uniaxial spin-glass

E. Gurewitz and U. Atzmony

Department of Physics, Nuclear Research Centre—Negev, P. O. Box 9001, Beer-Sheva, Israel

(Received 7 May 1982)

Mössbauer-effect studies were carried out on two mosaic samples of oriented single-crystal platelets of Fe_2TiO_5 . The experiments were done at various temperatures between 15 and 300 K. The low-temperature spectra indicated that the spins of the Fe^{3+} ions were parallel to the crystallographic c axis. Hyperfine splittings were observed at temperatures higher than the "transition temperature" detected by susceptibility measurements. The temperature dependence of the most probable hyperfine magnetic field shows a transition at the same temperature as the cusp in the susceptibility measurements. These features are interpreted in terms of relaxation phenomena.

I. INTRODUCTION

The anisotropic uniaxial spin-glass behavior of Fe_2TiO_5 below 55 K was previously reported.¹ The following experimental results were presented: (a) The magnetic susceptibility was strikingly anisotropic at low temperatures. The c -axis susceptibility exhibits a cusp at 55 K, whereas the other two axes' susceptibilities exhibit smooth paramagnetic behavior below and above 55 K. (b) Powder neutron-diffraction measurements did not reveal long-range magnetic ordering even at liquid-helium temperature. (c) Analysis of the room-temperature neutron diffraction indicated that Fe^{3+} and Ti^{4+} ions were essentially randomly distributed at the $8f$ and $4c$ sites of the $Cmcm$ (D_{2h}^{17}) space group. (d) No anomalies or peaks were revealed by either ultrasonic measurements of single-crystal or specific-heat measurements of powder of Fe_2TiO_5 in the temperature range $30 \leq T \leq 80$ K. (e) Mössbauer-effect measurements on mosaics of oriented single-crystal platelets showed hyperfine splitting at 16 K. From the spectra patterns it was definitely concluded that the hyperfine magnetic field (HMF) was aligned in the c direction.

In this paper we introduce the detailed Mössbauer-effect studies of Fe_2TiO_5 . Measurements were performed on powder sample and on two mosaic samples of oriented single-crystal platelets. The crystallographic c axes of the crystals were aligned parallel in one sample and perpendicular in the second sample to the direction of the γ radiation.

This paper contains analysis of the data in terms of field distribution, and it gives some qualitative description of the clustering of spins. Mössbauer-effect measurements on compounds with spin-glass

nature were previously reported.²⁻¹¹ A common feature of all the presented hyperfine split spectral patterns is their broad absorption lines, even at low temperatures. This broadening is attributed to two sources: (a) HMF distribution, namely a variety of HMF's, and (b) relaxation phenomena. The first source broadens mainly the outermost absorption lines, while the second source broadens mainly the innermost absorption lines. The analysis of the HMF distribution was done in some of these studies²⁻⁵ by the procedure proposed by Window,¹² other studies⁵⁻⁷ used step functions as proposed by Hesse and Rübartsch,¹³ and there are some studies¹¹ which assumed a known shape of the distribution of the HMF. In the present study the field distribution was expanded in Lorentzians. Clustering of the spins was explained by relaxation times and anisotropy. The Fe_2TiO_5 compound was the first to exhibit uniaxial spin-glass behavior.

II. EXPERIMENTAL

Single crystals of Fe_2TiO_5 with approximate dimensions of $8 \times 5 \times 3$ mm³ were grown by B. Wanklyn (Clarendon Laboratory, Oxford, England). These crystals were used to prepare two samples as follows: The crystals were cemented to a Perspex sheet with their c axes perpendicular in one sample [γ perpendicular to c (GPC) sample], and parallel in the second sample [γ vertical to c (GVC) sample]. The thickness of the crystals was reduced to the height of 100 μm above the Perspex sheets, which made them suitable to Mössbauer-effect measurements in transition geometry. The GPC and the GVC samples were designed for γ transition parallel and vertical to the c direction, respectively. Conventional ^{57}Fe Mössbauer spec-

trospectroscopy with a ^{57}Co -in-Pd source was used. The spectra were obtained using a constant-acceleration-type spectrometer. The absorber was cooled in a liquid-helium flow cryostat, and the temperature stability was within 0.5 K.

III. RESULTS AND DISCUSSION

A. Hyperfine magnetic field distribution analysis

Mössbauer spectra of a Fe_2TiO_5 powder sample at the temperatures of 15 and 28 K are shown in Fig. 1. The spectra exhibit six, well-defined but broadened, absorption lines. These patterns could not be fit by the usual six Lorentzians expected from a single set of equivalent positioned Fe^{3+} ions. As was established by neutron-diffraction measurements, the Fe^{3+} and Ti^{4+} ions are randomly distributed among the $8f$ and $4c$ special positions of the $Cmcm(D_{2h}^{17})$ space group. This random distribution yields a large number of structurally inequivalent Fe^{3+} sites. Therefore, Mössbauer absorption patterns of this compound should exhibit superposition of a large number of hyperfine splittings.

The main contributions to the HMF at a Mössbauer nucleus are due to its own ionic magnetic moment and to those of its nearest neighbors. The magnetic moment of the Fe^{3+} ions in this compound are either parallel or antiparallel to the c direction.¹ Consideration of nearest neighbors only limits the number of possible spin configurations

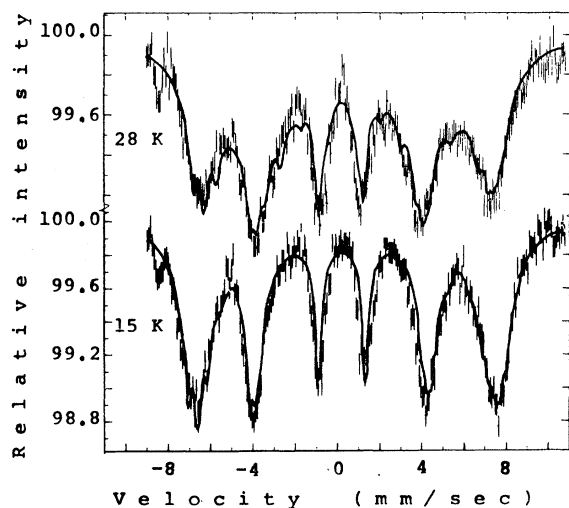


FIG. 1. Mössbauer spectra of a powder sample of Fe_2TiO_5 . The solid lines are the best-fit calculated spectra.

and therefore the number of HMF's. The contribution of further ions are taken into account as broadening of the HMF of each configuration to a distribution of HMF's.

The HMF distributions assumed in this work were Lorentzian distributions:

$$P_j(H) = \frac{4}{\pi} \frac{\Gamma_H(H_0)}{\Gamma_H^2(H_0) + 4(H - H_0)^2}.$$

Convolution of a Lorentzian distribution with Lorentzian absorption lines is

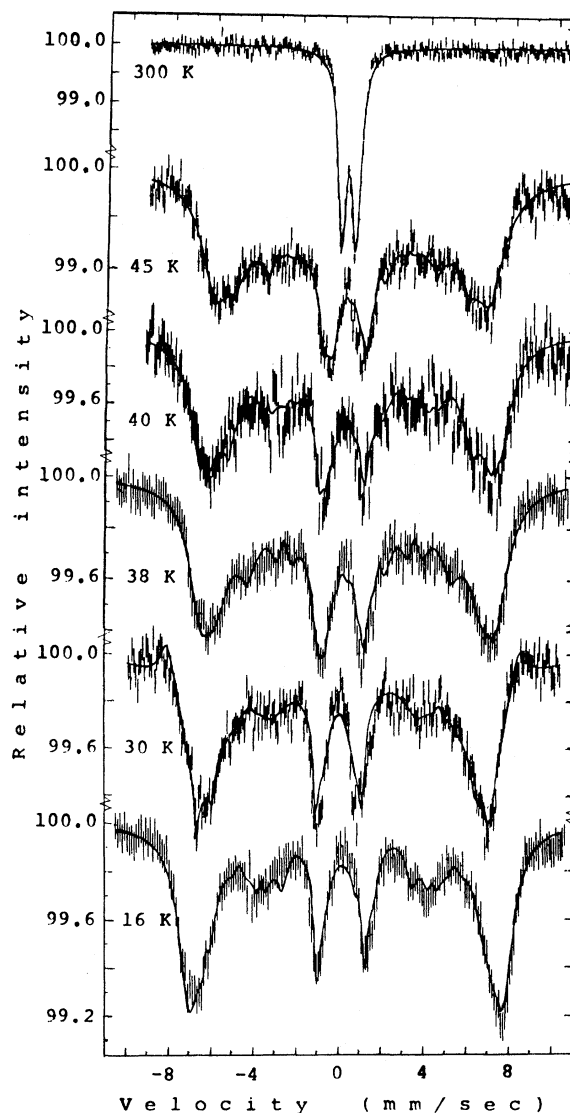


FIG. 2. Mössbauer spectra of a single-crystal sample of Fe_2TiO_5 . The c axes of the crystals are parallel to the direction of the measured γ radiation (GPC sample). The solid lines are the best-fit calculated spectra.

$$I_i(\omega) = \int_{-\infty}^{\infty} \frac{P_{\omega}^2(H)dH}{P_{\omega}^2(H) + 4[\omega_i(H) - \omega]^2}$$

$$= \frac{A_i(\Gamma + A_i)[h^2 + (A_i - \Gamma)^2]}{(A_i^2 - \Gamma^2 + h^2)^2 + 4A_i^2h^2},$$

$$A_i = \left| \frac{\Gamma_{\omega_i}}{2\gamma_i} \right|, \quad \Gamma = \frac{\Gamma_H}{2}, \quad i = 1, 2, 3, 4, 5, 6$$

$$h = H_0 - \frac{\omega - (-1)^i Q - \Delta_{\text{IS}}}{\Gamma_i},$$

$$\gamma_i = g_{3/2} m_{3/2}^i - g_{1/2} m_{1/2}^i,$$

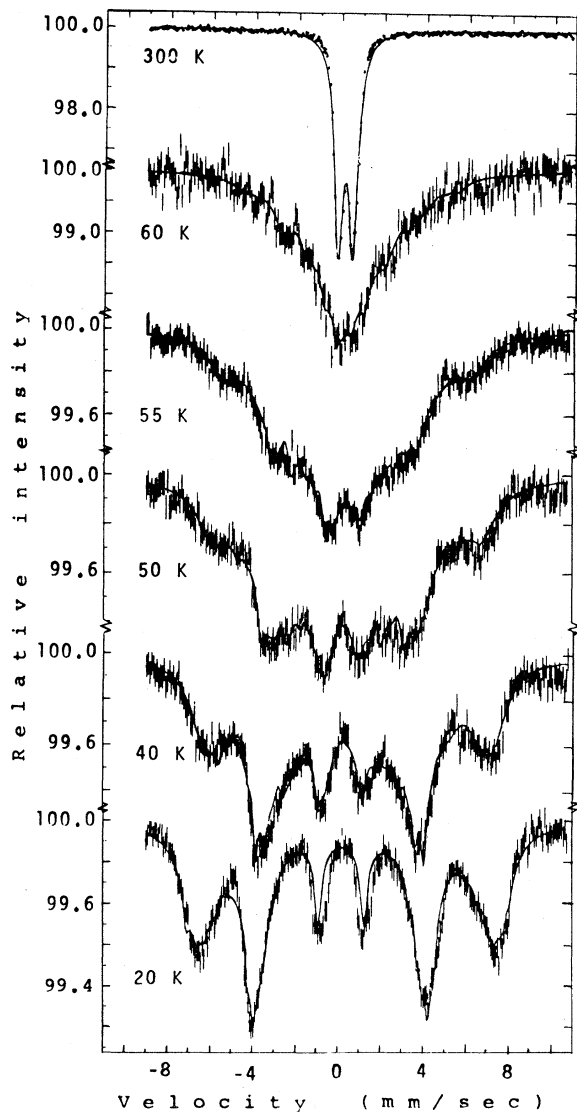


FIG. 3. Mössbauer spectra of a single-crystal sample of Fe_2TiO_5 . The c axes of the crystals are perpendicular to the direction of the measured γ radiation (GVC sample). The solid lines are the best-fit calculated spectra.

where g_i is the nuclear g factor for either nuclear levels $J = \frac{3}{2}$ or $J = \frac{1}{2}$, $Q = eqV_{zz}/4$ is the quadrupole energy parameter, Γ_{ω} and Γ_H are the Lorentzian halfwidths of the absorption line and the HMF distribution, respectively, H_0 is the center of a Lorentzian of the HMF distribution, and Δ_{IS} is the isomer shift.

The spectra, Figs. 1–3, were fitted by a least-squares program to HMF distributions composed of five such Lorentzians. The calculated patterns are shown by the solid line in the figures and the best-fit parameters are listed in Table I.

B. Magnetization axis

The relative intensities of the six absorption lines for the 14.4-keV transition in ^{57}Fe are¹⁴ $3y:1:1:y:3$, where

$$y = \sin^2\theta / (1 + \cos^2\theta)$$

and θ is the angle between the directions of the magnetic field and the emitted γ ray. For γ rays emitted parallel to the direction of the HMF, $y = 0$ and the absorption lines 2 and 5 vanish. This is exhibited by the spectra obtained from the GPC sample, Fig. 2. For γ rays emitted perpendicular to the HMF direction, $y = 4$ and the lines 2 and 5 are the strongest absorption lines. This is exhibited by the spectra obtained from the GVC sample, Fig. 3. This strictly indicated the c -uniaxial anisotropy which exists in Fe_2TiO_5 . This anisotropy was rigorously shown by susceptibility measurements.¹

The spectra patterns, Figs. 2 and 3, were fitted by a least-squares program to HMF distributions. The relative intensities of the six absorption lines, for each component of the HMF distribution, were $3:0:1:1:0:3$ and $3:4:1:1:4:3$ for the GPC, Fig. 2, and GVC, Fig. 3, respectively. The calculated spectra are shown by the solid lines in the figures.

C. Temperature dependence of the hyperfine magnetic field

The distributions of the HMF's at the various temperatures, as yielded by the least-squares best-fit procedure, are shown in Fig. 4. The peaks in these distributions are probably a result of the five-Lorentzian method used to unfold the distributions, though some peaks can describe a real feature of the distributions. The broken lines in Fig. 4 are a smooth line which cuts off the "extra peaks." Analysis of the data obtained from the GPC and the GVC samples yielded similar HMF distribu-

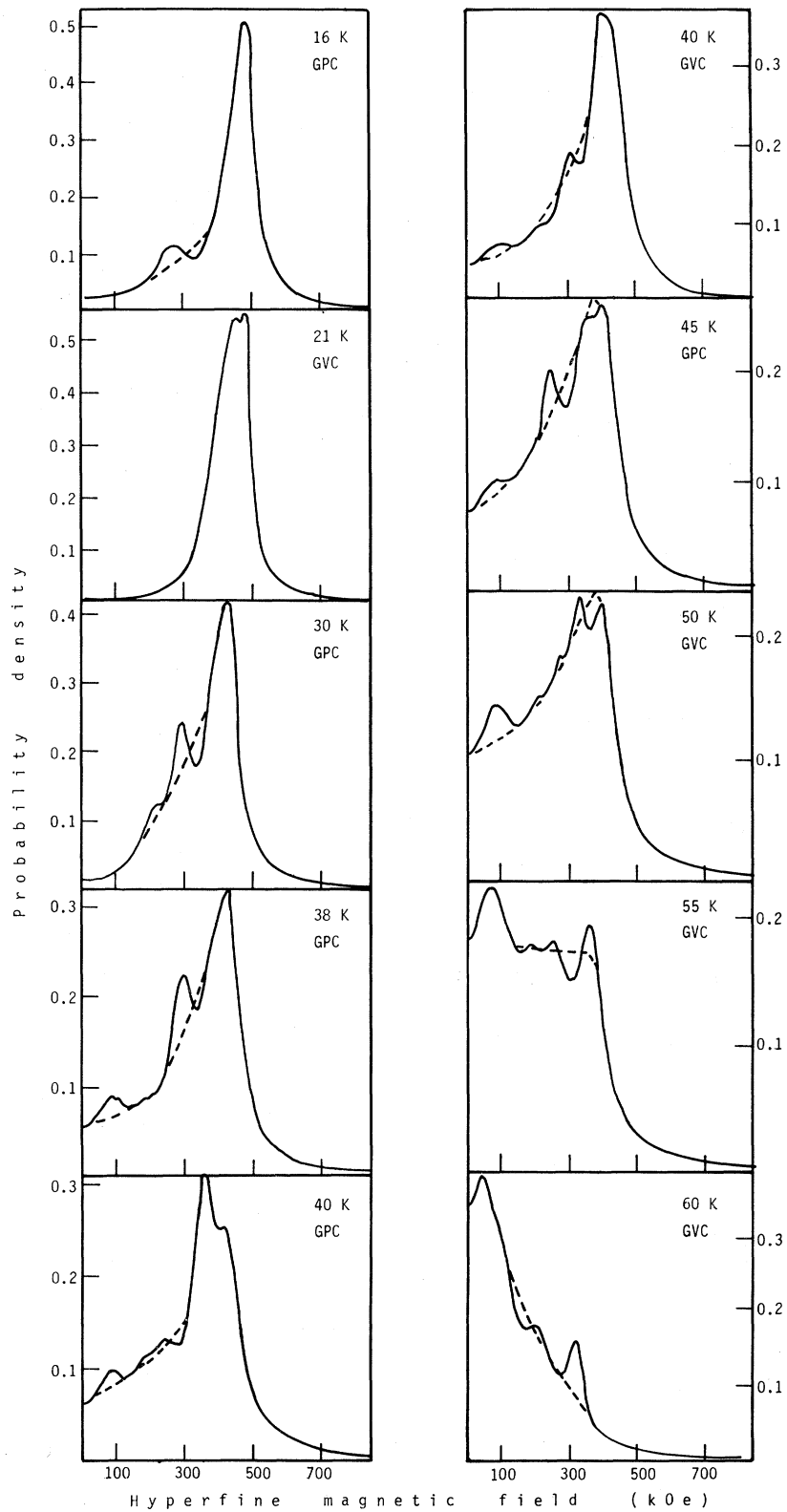


FIG. 4. Probability density of the hyperfine magnetic fields in Fe_2TiO_5 at various temperatures.

TABLE I. Values obtained by the best-fit procedure for the average HMF, \bar{H} , the most probable HMF, H_M , the width of the HMF distributions, W , quadrupole interaction, Δ_{IS} , and the width of the absorption line in the various temperatures.

T (K)	Sample type	\bar{H} (kOe)	H_M (kOe)	W (kOe)	$eqV_{zz}/4$ (mm/sec)	Δ_{IS} (mm/sec)	Γ_{ω} (mm/sec)
15	Powder	442±18	442±18	66±3	0.14±0.03	0.30±0.03	0.6
16	GPC	404±16	459±18	144±9	0.14±0.03	0.30±0.03	0.6
21	GVC	416±17	441±18	87±5	0.15±0.03	0.29±0.03	0.6
28	Powder	383±15	427±17	136±9	0.18±0.03	0.31±0.03	0.7
30	GPC	363±15	425±17	153±9	0.14±0.03	0.29±0.03	0.7
38	GPC	329±13	425±17	197±12	0.17±0.03	0.30±0.03	0.7
40	GPC	317±13	362±14	220±12	0.17±0.03	0.29±0.03	0.7
40	GVC	285±12	356±14	218±12	0.15±0.03	0.28±0.03	0.7
45	GPC	291±12	397±16	213±12	0.16±0.03	0.31±0.03	0.8
50	GVC	260±10	326±13	251±15	0.18±0.03	0.25±0.03	0.8
55	GVC	205±8	71±3	263±15	0.15±0.03	0.26±0.03	0.8
60	GVC	130±5	41±2	201±12	0.18±0.03	0.34±0.03	0.8

tions, Fig. 4. This increases the reliability of the obtained distributions.

At the lowest temperature the HMF distribution is the narrowest and is centered around 450 kOe. As temperature increases, the most probable HMF shifts slightly toward lower fields, and its intensity

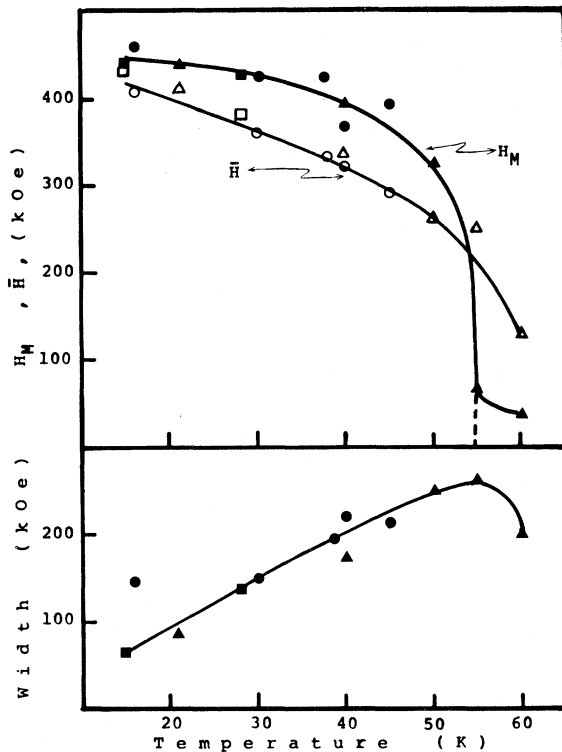


FIG. 5. Variation with temperature of the average HMF, \bar{H} , the most probable HMF, H_M , and the width of the HMF distributions. Circles are for the GPC, triangles for GVC, and squares for the powder sample.

decreases while the intensity of the low-field side of the distribution increases. At about 55 K there is a broad distribution with almost equal probability but a slight preference to fields which are close to zero. At higher temperatures the most probable field is close to zero and the distribution has a higher-field tail which narrows with temperature. The three following parameters, characterizing the distributions, are defined:

(a) The average HMF, $\bar{H} = \sum_{i=1}^5 H_0^i I^i$, where H_0^i is the center of the i th Lorentzian and I^i is its relative weight in the distribution, $\sum_{i=1}^5 I^i = 1$.

(b) The width W of the distribution, $W = H_2 - H_1$, where

$$\int_{-\infty}^{H_1} P(H) dH = \int_{H_2}^{\infty} P(H) dH = \frac{1}{4}.$$

(c) The most probable field H_M , i.e., the field for which $P(H)$ has its maximum.

The variation of these parameters with temperature are shown in Fig. 5. The most probable field H_M , at temperatures lower than 50 K, is higher than \bar{H} . At $T = 55$ K, H_M drops abruptly almost to zero and above this temperature it has a "short-range-order-like" tail. It should be noticed that 55 K is also the temperature of the cusp in the susceptibility measurements of Fe_2TiO_5 .¹ The susceptibility, as well as the most probable field H_M , is dominated by the large magnetic clusters. Therefore the temperature of the cusp in the susceptibility corresponds to the "transition" temperature in H_M .

Mössbauer-effect measurements show the existence of HMF at temperatures higher than 55 K,

but not higher than 70 K. Furthermore, neutron-diffraction scans of Fe_2TiO_5 single crystal revealed magnetic correlations at temperatures as high as room temperature.¹⁵ Such differences between the freezing temperatures obtained by these three kinds of measurements were described by Murani.^{16,17} These differences fit the model of Smith¹⁸ for spin-glasses. Smith's model defined clusters of correlated spins. All the spins in a cluster are completely aligned, and each cluster is free to rotate as a rigid body in the presence of the other clusters.

The Fe_2TiO_5 strong anisotropy restricts its spins to the $\pm c$ direction. Therefore, the clusters flip between the $+c$ and $-c$ directions. The relaxation times of the clusters as function of temperature and anisotropy are given by $\tau = \tau_0 e^{E_a/kT}$, where E_a is the anisotropy of the cluster and τ_0 is its intrinsic relaxation time. This expression was originally introduced by Néel¹⁹ for superparamagnetic particles. When the temperature decreases, the relaxation times and the time-average magnetization $\langle S \rangle_\tau$ increase. The increase in $\langle S \rangle_\tau$ causes the merging of clusters into larger clusters of spins. When the relaxation time of a cluster reaches the order of magnitude of the Larmor precession period, a magnetic hyperfine splitting is observable by Mössbauer-effect measurements. According to this model, a measurement will show a transition when the relaxation time exceeds the duration of this measurement.²⁰

The influence of the relaxation on the Mössbauer spectra were accounted for by broadening the Lorentzian absorption lines. More sophisticated calculations, such as those done for KFeCl_3 ,²¹ did not improve the fit appreciably.

D. Quadrupole interaction and isomer shift

In the procedure of best-fitting calculated spectra to the observed data, an average quadrupole interaction and isomer shift were assumed. According to Table I, the best-fit values for these averages did not change much with temperature. The spectra observed at room temperature did not exhibit any variety of either quadrupole interaction or isomer shift. This justifies the use of average values for these two parameters. Although the Fe^{3+} ions are located at a variety of crystallographic environments, a single quadrupole splitting is observed. Consequently, the electric field gradient is not sensitive to this variation.

The isomer shifts have the Fe^{3+} value. It is consistent with the fact that Fe^{2+} HMF splitting was not observed. This should be emphasized because the Fe_2TiO_5 compound could contain some Fe_2TiO_4 impurity.

ACKNOWLEDGMENTS

The authors are grateful to Professor G. Gorodetzky of Ben Gurion University of the Negev for preparing the samples. Gratitude is expressed to Mrs. B. M. Wanklyn of Clarendon Laboratory, Oxford, for supplying the single crystals. Thanks are due to Professor H. Shaked and Mr. H. Pinto of the Nuclear Research Centre—Negev and Professor R. M. Hornreich of the Weizmann Institute of Science for stimulating discussions.

¹U. Atzmony, E. Gurewitz, M. Melamud, H. Pinto, H. Shaked, G. Gorodetzky, R. M. Hornreich, S. Shtrikman, and B. Wanklyn, *Phys. Rev. Lett.* **43**, 789 (1979).
²C. L. Chien, *Phys. Rev. B* **18**, 1003 (1978).
³C. L. Chien, D. Musser, F. E. Luborsky, and J. L. Walter, *Metal Phys.* **8**, 2407 (1978).
⁴M. C. Lin, C. S. Serverin, R. G. Barnes, and C. W. Chen, *Phys. Rev. B* **24**, 3719 (1981).
⁵C. L. Chien, D. Musser, E. M. Gyorgy, R. C. Sherwood, H. S. Chen, F. E. Luborsky, and J. L. Walter, *Phys. Rev. B* **20**, 283 (1979).
⁶I. Vincze, *Solid State Commun.* **25**, 689 (1978).
⁷T. Kemeny, I. Vincze, B. Forgarassy, and S. Arajs, *Phys. Rev. B* **20**, 476 (1979).
⁸W. Kurtz, R. Geller, H. Dachs, and P. Convert, *Solid State Commun.* **18**, 1479 (1976).
⁹R. Abbundi, J. J. Rhyne, D. M. Sweger, and R. Segnam,

Phys. Rev. B **18**, 3313 (1978).
¹⁰A. Wiedmann, P. Burlet, and R. Chevotier, *J. Magn. Magn. Mater.* **15-18**, 216 (1980).
¹¹E. Sharon and C. C. Tsuei, *Phys. Rev. B* **5**, 1047 (1972).
¹²B. Window, *J. Phys. E* **4**, 401 (1971).
¹³J. Hesse and A. Rübartsch, *J. Phys. E* **7**, 526 (1974).
¹⁴G. K. Wertheim, *Mössbauer Effect Principles and Applications* (Academic, New York, 1964), p. 75.
¹⁵E. Gurewitz, H. Pinto, and H. Shaked (unpublished).
¹⁶A. P. Murani, *Phys. Rev. Lett.* **37**, 450 (1976).
¹⁷A. P. Murani, *J. Magn. Magn. Mater.* **5**, 95 (1977).
¹⁸D. A. Smith, *J. Phys. F* **4**, L266 (1974).
¹⁹L. Néel, *C. R. Acad. Sci.* **228**, 664 (1949).
²⁰P. Mears, *Polymers Structure and Bulk Properties* (Van Nostrand, London, 1965), Chap. 10.
²¹E. Gurewitz, J. Makovsky, and U. Atzmony, *Phys. Rev. B* **13**, 375 (1976).